Dissociation of heavy quarkonia in an anisotropic hot QCD medium in a quasiparticle model

Mohammad Yousuf Jamal,[1,*] Indrani Nilima,[2,†] Vinod Chandra,[1,‡] and Vineet Kumar Agotiya[2,§]

[1]*Indian Institute of Technology Gandhinagar, Gandhinagar, Gujarat 382 355, India*

[2]*Centre for Applied Physics, Central University of Jharkhand, Ranchi, Jharkhand 835 205, India*

(Received 12 February 2018; published 31 May 2018)

The present article is the follow-up work of Phys. Rev. D **94**, 094006 (2016), where we have extended the study of quarkonia dissociation in (momentum) anisotropic hot QCD medium. As evident by the experimentally observed collective flow at the RHIC and LHC, the momentum anisotropy is present at almost all the stages after the collision, and therefore, it is important to include its effects in the analysis. Employing the in-medium (corrected) potential while considering the anisotropy (both oblate and prolate cases) in the medium, the thermal widths and the binding energies of the heavy quarkonia states (s-wave charmonia and s-wave bottomonia specifically, for radial quantum numbers $n = 1$ and 2) have been determined. The hot QCD medium effects have been included by employing a quasiparticle description. The presence of anisotropy has modified the potential and then the thermal widths and binding energies of these states in a significant manner. The results show a quite visible shift in the values of dissociation temperatures as compared to the isotropic case. Further, the hot QCD medium interaction effects suppress the dissociation temperature as compared to the case where we consider the medium as a noninteracting ultrarelativistic gas of quarks (antiquarks) and gluons.

DOI: 10.1103/PhysRevD.97.094033

I. INTRODUCTION

In the ultrarelativistic heavy-ion collision experiments at the RHIC and LHC, it has been inferred that the quark-gluon-plasma (QGP) formed functions more like a perfect fluid rather than a noninteracting ultrarelativistic gas of quarks (antiquarks) and gluons [1–3]. This is because of the fact that the QGP possesses a robust collective property that could be quantified in terms of the flow harmonics. Among the other important signatures based on the experimental observations, quarkonia ($Q\bar{Q}$) suppression has also been suggested as a clear probe of the QGP formation in the collider experiments [4,5]. As observed in the experiments, it accentuates the plasma aspects of the medium, for example, Landau damping [5], color screening [6], and the energy loss [7].

After the discovery of J/ψ (a bound state of $c\bar{c}$) [8,9], in 1974, both the experimental and the theoretical studies of heavy quarkonia have become interesting topics for researchers to investigate. A pioneering research, the dissociation of quarkonia due to the color screening in the deconfined medium with finite temperature, was first carried out by Matsui and Satz [10]. Thereafter, a large number of excellent articles have been published that envisioned several essential refinements in the study of quarkonia [11–15].

Quarkonium is the color singlet and the flavorless state of the heavy quark-antiquark bound together by almost static gluons [16–18]; it is mainly produced at the very early stages, just after the collisions of the ultrarelativistic nuclei, and it acts as an independent degree of freedom. While traversing through the medium, quarkonia also make transitions to other quarkonia states with the emission of light hadrons [19]. Being bound states of $Q\bar{Q}$, heavy quarkonia also provide a possibility to explore the important features of quantum chromodynamics (QCD), the theory of strong interactions, due to the presence of various scales [20–22], at high temperatures. Quarkonia production in the hot QCD medium has been studied in several works. In this context, the color evaporation model [23–26] is motivated by the principle of quark-hadron duality; i.e., it assumes that every $c\bar{c}$ produced evolves into charmonium if it has an invariant mass less than the threshold for producing a pair of open charm mesons. On the other hand, the quarkonia production in the color singlet mechanism has been studied in Refs. [26–28], whereas the enhancement in the production or suppression of quarkonia through coalescence or the recombination of the quarks or antiquarks has been discussed in Refs. [29,30].

As the heavy quark masses, m_c or $m_b \gg \Lambda_{\rm QCD}$ (QCD scale), the velocity of the bound states of heavy quarks

*mohammad.yousuf@iitgn.ac.in
†nilima.ism@gmail.com
‡vchandra@iitgn.ac.in
§agotiya81@gmail.com

remains small, and hence, the nonrelativistic QCD (NRQCD) approach [31–34], using nonrelativistic potential models, has also been exploited in the present context. In this approach, the potential between heavy quarkonia must be approximated by the short-distance Coulombic effects (which satisfy asymptotic freedom) and the large-distance confinement effects. To that end, the Cornell potential is one of the first possibilities [35–37] to fulfill these requirements and describe the interaction between the heavy quark-antiquark pair. Recently, the properties of heavy quarkonia have been examined by several authors [38–40]. In particular, the production or suppression of quarkonia has been studied either theoretically or experimentally in Refs. [41–57], and the disassociation temperature has been studied in Refs. [58–64].

Following our recent work on dissociation of heavy quarkonia, within the quasiparticle approach, for the isotropic medium in Ref. [65], the present analysis accommodates the presence of local momentum anisotropy to estimate the dissociation temperature of heavy quarkonia. While considering the momentum anisotropy, both the oblate and the prolate situations have been taken into account and compared with the isotropic one. The motivation to incorporate the anisotropy in the study of quarkonia suppression comes from the fact that the QGP produced in heavy-ion (off-central) collisions does not possess isotropy. Instead, the momentum anisotropy is present in all the stages of the heavy-ion collisions, and hence, the inclusion of the anisotropy is inevitable. There are many articles [66–71] in which the impact of the anisotropy in various observables of QGP has been investigated. In most of these studies, the ideal Bose/Fermi distributions [72] have been considered in a combination to define the distribution function in an isotropic medium.

Considering the medium as a hot thermal bath instead of a noninteracting ideal one, we employ the effective fugacity quasiparticle distribution functions to incorporate the hot medium effects, using the effective fugacity quasiparticle model (EQPM) [73,74] for the isotropic medium. The anisotropy has been introduced at the level of the distribution function by stretching and squeezing it in one of the directions, as in Refs. [16,75–77]. The gluon propagator—and, in turn, the dielectric permittivity in the presence of anisotropy—in the hot QCD medium has been obtained using the gluon self-energy. We first calculate the real part and imaginary part of the in-medium Cornell potential, modified using dielectric permittivity, in Fourier space. The thermal width and the binding energy of quarkonia bound states are then determined by the imaginary and real parts of the modified potential [18,78–82], respectively. The dissociation temperatures have been calculated by exploiting the criterion [83–86], which says that, at the dissociation temperature, the thermal width equals twice the (real part of the) binding energy. To examine the hot QCD medium effects using EQPM [73,74], the hot QCD equations of state (EoSs) have been updated with the recent lattice [87,88], as well as 3-loop Hard Thermal Loop (HTL) perturbative [89,90] calculations.

The effects of anisotropy will modify the in-medium potential and, in turn, significantly revise the values of the dissociation temperature. In the oblate case, the dissociation temperature is observed to be higher than the isotropic case. In the prolate case, it is observed to be the least among the three cases. The tightly bound ground state has higher binding energies and is expected to melt later than the excited state; hence, it must have a sequential suppression pattern with temperature. The order observed in the present analysis supports the above fact as Υ' ($2s$-state of $b\bar{b}$) has been suppressed at smaller temperatures than the Υ ($1s$-state of $b\bar{b}$), for all considered EoSs. It can be further seen that the dissociation temperatures using nonideal EoSs are smaller than the ideal one for each $Q\bar{Q}$-state studied here.

The paper is organized as follows. In Sec. II, we review the heavy-quark potential with its real and imaginary parts in the anisotropic medium. We describe the quasiparticle model that has been employed in our analysis and discuss the binding energy and melting of heavy quarkonia states. Section III includes our results and a discussion. In Sec. IV, we conclude the present work.

II. HEAVY-QUARK POTENTIAL, THERMAL WIDTH AND QUARKONIA BINDING ENERGY IN THE ANISOTROPIC HOT QCD MEDIUM

The crucial role played by the static heavy-quark potential to understand the physics behind the quarkonia bound state has been studied by several authors as mentioned earlier. In the present analysis, we prefer to work with the Cornell potential [35,36], which contains the Coulombic as well as the string part, given as

$$\mathrm{V}(r) = -\frac{\alpha}{r} + \sigma r, \tag{1}$$

modifying it in the presence of a dissipative medium using the dielectric permittivity $\epsilon(k)$ in Fourier space. Here, r is the effective radius of the corresponding quarkonia state, α is the strong coupling constant, and σ is the string tension. The modification of the string part along with the Coulombic part can be exploited due to the fact that the transition from the hadronic phase to the QGP is a crossover [91], so the string tension does not vanish abruptly at or near T_c. Let us now briefly discuss the EQPM [73,74] and then describe the medium modification of the above potential in the presence of anisotropy. After that, we address the binding energy and thermal width using the derived modified potential.

A. EQPM and Debye screening

EQPM maps the hot QCD medium effects with the effective equilibrium distribution function $f_{g,q}(p)$ of

quasipartons [73,74], which describes the strong interaction effects in terms of effective fugacities, $z_{g,q}$. Here, the quasiparton equilibrium distribution functions for the gluon and quark/antiquark, respectively, read as

$$f_g(p) = \frac{1}{z_g^{-1} e^{\beta E_p} - 1}, \qquad f_{q/\bar{q}}(p) = \frac{1}{z_{q/\bar{q}}^{-1} e^{\beta E_p} + 1}. \quad (2)$$

Using EQPM, the energy dispersion relation is modified as

$$\omega_{g/q,\bar{q}} = E_p + T^2 \partial_T \ln(z_{g/q,\bar{q}}).$$

The Debye mass m_D can be obtained using the distribution functions given in Eq. (2) as

$$m_D^2 = -4\pi\alpha(T)\left(2N_c \int \frac{d^3p}{(2\pi)^3} \partial_p f_g(\mathbf{p}) + 2N_f \int \frac{d^3p}{(2\pi)^3} \partial_p f_q(\mathbf{p})\right), \quad (3)$$

where $\alpha(T)$ is the running coupling at finite temperature (T) [92]. Note that N_c and N_f are the color degrees of freedom and the number of flavors, respectively. Applying the quasiparton equilibrium distribution function from Eq. (2) in Eq. (3), we have

$$m_D^{2\,(EoS(i))} = 4\pi\alpha(T)T^2\left(\frac{2N_c}{\pi^2} PolyLog[2, z_g^i] - \frac{2N_f}{\pi^2} PolyLog[2, -z_q^i]\right), \quad (4)$$

where the index i denotes the different EoSs, incorporating the QCD interactions modeled from improved perturbative 3-loop HTL QCD computations by Haque *et al.* [89,90] and recent $(2+1)$-flavor lattice QCD simulations [87,88].

The weak perturbative (resummed) computations on the EoS in hot QCD show nice convergence properties and agree well with the lattice QCD results. The strong interaction effects encoded in lattice EoS (LEoS) could be applied to effective gluonic and quark/antiquark degrees of freedom and could be utilized to develop effective transport theory in those regions where weak perturbative results make sense, and transport theory could lead to reliable outcomes. The above work is performed in the above-mentioned spirit. In other words, with EQPM for LEoS, we cannot go much closer to T_c; the analysis is reliable beyond T_c ($T \gtrsim T_c$). Neither EQPM nor effective (linearized) transport theory methods will work very close to T_c. However, in the above-mentioned temperature, these methods could be used to take care of the interaction in an effective way. Working at the temperature $T = 3T_c$, we have studied the interaction effects which are important and were not considered in earlier work in this field.

In the limit, $z_{g,q} \to 1$, the m_D reduces to the leading order (LO) or ideal case, given as

$$m_D^{2\,(LO)} = 4\pi\alpha(T)T^2\left(\frac{N_c}{3} + \frac{N_f}{6}\right). \quad (5)$$

Let us now discuss the modification of the potential, considering the presence of anisotropy in the hot QCD medium.

B. Medium modified heavy-quark potential in the presence of anisotropy

Here, the anisotropy is introduced due to the fact that in the off-central relativistic heavy-ion collisions, the spatial anisotropy is generated at the very primary stages. As the system evolves with time, different pressure gradients are produced in different directions, which maps the spatial anisotropy to the momentum anisotropy. The anisotropy in the present formalism has been introduced at the particle phase-space distribution level. Employing the method used in Refs. [75–77], the anisotropic distribution function has been obtained from the isotropic one by rescaling (stretching and squeezing) it in one of the directions in momentum space as

$$f(\mathbf{p}) \to f_\xi(\mathbf{p}) = C_\xi f\left(\sqrt{\mathbf{p}^2 + \xi(\mathbf{p}\cdot\hat{\mathbf{n}})^2}\right), \quad (6)$$

where $f(\mathbf{p})$ is the effective fugacity quasiparticle distribution function for the isotropic medium [73,74]. The $\hat{\mathbf{n}}$ is a unit vector ($\hat{\mathbf{n}}^2 = 1$), showing the direction of momentum anisotropy. The parameter ξ gives the anisotropic strength in the medium and describes the amount of squeezing ($\xi > 0$, or oblate form) and stretching ($-1 < \xi < 0$, or prolate form) in the $\hat{\mathbf{n}}$ direction. Since the EoS effects enter through the Debye mass (m_D), we want to make it immune from the effects of anisotropy present in the medium so that it remains the same in both mediums (isotropic and anisotropic), as done in Ref. [76]. In doing so, only the effects of different EoSs will be carried in the m_D, and hence, the normalization constant C_ξ becomes

$$C_\xi = \begin{cases} \frac{\sqrt{|\xi|}}{\tanh^{-1}\sqrt{|\xi|}} & \text{if } -1 \le \xi < 0 \\ \frac{\sqrt{\xi}}{\tan^{-1}\sqrt{\xi}} & \text{if } \xi \ge 0. \end{cases} \quad (7)$$

In the small ξ limit, we have

$$C_\xi = \begin{cases} 1 - \frac{\xi}{3} + O(\xi^{\frac{3}{2}}) & \text{if } -1 \le \xi < 0 \\ 1 + \frac{\xi}{3} + O(\xi^{\frac{3}{2}}) & \text{if } \xi \ge 0. \end{cases} \quad (8)$$

To modify the potential due to the presence of the dissipative anisotropic hot QCD medium, the assumption

given in Ref. [12] has been followed, which says that the in-medium modification can be obtained in Fourier space by dividing the heavy-quark potential by the medium dielectric permittivity $\epsilon(\mathbf{k})$ as

$$\grave{V}(k) = \frac{\bar{V}(k)}{\epsilon(k)}. \tag{9}$$

By making the inverse Fourier transform, we can obtain the modified (or in-medium corrected) potential as

$$V(r) = \int \frac{d^3\mathbf{k}}{(2\pi)^{3/2}}(e^{i\mathbf{k}\cdot\mathbf{r}} - 1)\grave{V}(k), \tag{10}$$

where $\bar{V}(k)$ is the Fourier transform of $V(r)$, shown in Eq. (1), given as

$$\bar{V}(k) = -\sqrt{\frac{2}{\pi}}\left(\frac{\alpha}{k^2} + 2\frac{\sigma}{k^4}\right). \tag{11}$$

Next, to modify the potential, we first need to calculate the dielectric permittivity, which is obtained from the self-energy using finite temperature QCD. It is important to note that the perturbative theory at $T > 0$ suffers from the infrared singularities and gauge-dependent results because the perturbative expansion is incomplete at $T > 0$. There are infinitely many higher order diagrams with more and more loops that can contribute to lower order in the coupling constant [93]. This problem can be partly avoided by using the HTL resummation technique [94], and one can obtain consistent results up to the leading order. Another equivalent approach to obtain $\epsilon(\mathbf{k})$ is the many-particle kinetic theory (or the semiclassical transport theory), which provides the same results up to one-loop order (or in the Abelian limit) [77,95,96]. Exploiting any of these two methods, one finds the gluon self-energy $\Pi^{\mu\nu}$ and then the static gluon propagator that represents the inelastic scattering of an off-shell gluon to a thermal gluon,

$$\Delta^{\mu\nu}(\omega, \mathbf{k}) = k^2 g^{\mu\nu} - k^\mu k^\nu + \Pi^{\mu\nu}(\omega, \mathbf{k}). \tag{12}$$

Next, the dielectric tensor can be obtained in the static limit, in Fourier space, from the temporal component of the propagator, as

$$\epsilon^{-1}(\mathbf{k}) = -\lim_{\omega\to 0} k^2 \Delta^{00}(\omega, \mathbf{k}). \tag{13}$$

Now, to obtain the real part of the interquark potential in the static limit, the temporal component of the real part of the retarded (or advanced) propagator in Fourier space is needed, which is given as

$$\mathrm{Re}[\Delta^{00}_{R(A)}](\omega = 0, \mathbf{k}) = \frac{-1}{k^2 + m_D^2} - \xi\left(\frac{1}{3(k^2 + m_D^2)} - \frac{m_D^2(3\cos 2\theta_n - 1)}{6(k^2 + m_D^2)^2}\right). \tag{14}$$

The imaginary part can be derived from the imaginary part of the temporal component of the symmetric propagator in the static limit:

$$\mathrm{Im}[\Delta^{00}_S](\omega = 0, \mathbf{k}) = \pi T m_D^2\left(\frac{-1}{k(k^2 + m_D^2)^2} + \xi\left(\frac{-1}{3k(k^2 + m_D^2)^2} + \frac{3\sin^2\theta_n}{4k(k^2 + m_D^2)^2} - \frac{2m_D^2(3\sin^2(\theta_n) - 1)}{3k(k^2 + m_D^2)^3}\right)\right), \tag{15}$$

where

$$\cos(\theta_n) = \cos(\theta_r)\cos(\theta_{pr}) + \sin(\theta_r)\sin(\theta_{pr})\cos(\phi_{pr}). \tag{16}$$

In the above expression, the angle θ_n is in between the particle momentum $\mathbf{p}$ and the direction of anisotropy, $\hat{\mathbf{n}}$. The angle between $\mathbf{r}$ and $\mathbf{n}$ is θ_r. Note that ϕ_{pr} and θ_{pr} are, respectively, the azimuthal and the polar angle between $\mathbf{p}$ and $\mathbf{r}$. Next, to modify the real part of the potential, $\epsilon(\mathbf{k})$ can be obtained using Eq. (14) in Eq. (13) as

$$\epsilon^{-1}(\mathbf{k}) = \frac{k^2}{k^2 + m_D^2} + k^2\xi\left(\frac{1}{3(k^2 + m_D^2)} - \frac{m_D^2(3\cos 2\theta_n - 1)}{6(k^2 + m_D^2)^2}\right). \tag{17}$$

Similarly, the imaginary part of the potential can be modified by using $\epsilon(\mathbf{k})$, which can be obtained by employing Eq. (15) in Eq. (13) as

$$\epsilon^{-1}(\mathbf{k}) = \pi T m_D^2\left(\frac{k^2}{k(k^2 + m_D^2)^2} - \xi k^2\left(\frac{-1}{3k(k^2 + m_D^2)^2} + \frac{3\sin^2\theta_n}{4k(k^2 + m_D^2)^2} - \frac{2m_D^2(3\sin^2(\theta_n) - 1)}{3k(k^2 + m_D^2)^3}\right)\right). \tag{18}$$

In the limit $T \to 0$, and in the absence of anisotropy, the real part of $\epsilon^{-1}(k)$ goes to unity, while the imaginary part vanishes; thus, the modified potential simply reduces to the Cornell form. In the next two subsections, we discuss the real and imaginary potentials, modified using the above-defined $\epsilon^{-1}(\mathbf{k})$.

1. Real part of the potential in the anisotropic medium

Using Eq. (17) in Eq. (10), we can write the real part of the potential as

$$\mathrm{Re}[V(\mathbf{r},\xi,T)] = \int \frac{d^3\mathbf{k}}{(2\pi)^{3/2}}(e^{i\mathbf{k}\cdot\mathbf{r}}-1)\left(-\sqrt{\frac{2}{\pi}}\frac{\alpha}{k^2}-\frac{4\sigma}{\sqrt{2\pi}k^4}\right)\left(\frac{k^2}{k^2+m_D^2}+k^2\xi\left(\frac{1}{3(k^2+m_D^2)}-\frac{m_D^2(3\cos 2\theta_n-1)}{6(k^2+m_D^2)^2}\right)\right). \quad (19)$$

Solving the above integral, we find

$$\begin{aligned}\mathrm{Re}[V(\mathbf{r},\xi,T)] = {}& \alpha m_D\left(-\frac{e^{-s}}{s}-1\right)+\frac{\sigma}{m_D}\left(\frac{2e^{-s}}{s}-\frac{2}{s}+2\right)\\ &+\alpha\xi m_D\left[-\frac{3\cos(2\theta_r)}{2s^3}-\frac{1}{2s^3}+\frac{1}{6}+e^{-s}\left\{\frac{1}{2s^3}+\frac{1}{2s^2}+\left(\frac{3}{2s^3}+\frac{3}{2s^2}+\frac{3}{4s}+\frac{1}{4}\right)\cos(2\theta_r)+\frac{1}{4s}-\frac{1}{12}\right\}\right]\\ &+\frac{\xi\sigma}{m_D}\left[\left(\frac{6}{s^3}-\frac{1}{2s}\right)\cos(2\theta_r)+\frac{2}{s^3}-\frac{5}{6s}+\frac{1}{3}+e^{-s}\left\{-\frac{2}{s^3}-\frac{2}{s^2}+\left(-\frac{6}{s^3}-\frac{6}{s^2}-\frac{5}{2s}-\frac{1}{2}\right)\cos(2\theta_r)-\frac{1}{6s}+\frac{1}{6}\right\}\right]\end{aligned} \quad (20)$$

where $s = rm_D$. Considering the limit $s \ll 1$ in Eq. (20), we have

$$\begin{aligned}\mathrm{Re}[V(\mathbf{r},\xi,T)] = {}& \frac{s\sigma}{m_D}\left(1+\frac{\xi}{3}\right)-\frac{\alpha m_D}{s}\left(1+\frac{s^2}{2}\right.\\ &\left.+\xi\left(\frac{1}{3}+\frac{s^2}{16}\left(\frac{1}{3}+\cos(2\theta_r)\right)\right)\right).\end{aligned} \quad (21)$$

Here, in the isotropic limit, one can observe that there is an additional term in s with α in Eq. (21). This term vanishes in the limit $T \to 0$, and we end up with the vacuum potential; however, it contributes as a thermal correction to the real part of the medium modified potential at $T \neq 0$.

2. Imaginary part of the potential in the anisotropic medium

The imaginary potential, using Eq. (18) in Eq. (10), can be written as

$$\begin{aligned}\mathrm{Im}[V(\mathbf{r},\xi,T)] = {}& \pi T m_D^2\int\frac{d^3\mathbf{k}}{(2\pi)^{3/2}}(e^{i\mathbf{k}\cdot\mathbf{r}}-1)\left(-\sqrt{\frac{2}{\pi}}\frac{\alpha}{k^2}\right.\\ &\left.-\frac{4\sigma}{\sqrt{2\pi}k^4}\right)\left(\frac{k}{(k^2+m_D^2)^2}-\xi\left(\frac{-k}{3(k^2+m_D^2)^2}\right.\right.\\ &\left.\left.+\frac{3k\sin^2\theta_n}{4(k^2+m_D^2)^2}-\frac{2m_D^2k(3\sin^2(\theta_n)-1)}{3(k^2+m_D^2)^3}\right)\right).\end{aligned} \quad (22)$$

To solve the above equation, we separate the Coulombic term (containing α) and the string term (having σ) as

$$\mathrm{Im}[V(\mathbf{r},\xi,T)] = \mathrm{Im}V_1(\mathbf{r},\xi,T)+\mathrm{Im}V_2(\mathbf{r},\xi,T). \quad (23)$$

$$\begin{aligned}\mathrm{Im}V_1(\mathbf{r},\xi,T) = {}& \frac{\alpha T m_D^2}{2\pi}\int d^3\mathbf{k}(e^{i\mathbf{k}\cdot\mathbf{r}}-1)\frac{1}{k}\left[\frac{-1}{(k^2+m_D^2)^2}\right.\\ &+\xi\left[\frac{-1}{3(k^2+m_D^2)^2}+\frac{3\sin^2\theta_n}{2(k^2+m_D^2)^2}\right.\\ &\left.\left.-\frac{4m_D^2(\sin^2\theta_n-\frac{1}{3})}{(k^2+m_D^2)^3}\right]\right]\end{aligned} \quad (24)$$

and

$$\begin{aligned}\mathrm{Im}V_2(\mathbf{r},\xi,T) = {}& \frac{\sigma T m_D^2}{\pi}\int d^3\mathbf{k}(e^{i\mathbf{k}\cdot\mathbf{r}}-1)\frac{1}{k^3}\left[\frac{-1}{(k^2+m_D^2)^2}\right.\\ &+\xi\left[\frac{-1}{3(k^2+m_D^2)^2}+\frac{3\sin^2\theta_n}{2(k^2+m_D^2)^2}\right.\\ &\left.\left.-\frac{4m_D^2(\sin^2\theta_n-\frac{1}{3})}{(k^2+m_D^2)^3}\right]\right].\end{aligned} \quad (25)$$

The contribution due to the Coulombic part in the imaginary potential considering the limit $rm_D \equiv s \ll 1$ is found to be

$$\mathrm{Im}V_1(r,\theta_r,T) = -\frac{\alpha s^2 T}{180}\{\xi(9\cos 2\theta_r-7)+60\}\log\left(\frac{1}{s}\right), \quad (26)$$

and from the string part, we obtain

$$\mathrm{Im}V_2(r,\theta_r,T) = -\frac{s^4\sigma T}{1260m_D^2}\{\xi(9\cos 2\theta_r-4)+42\}\log\left(\frac{1}{s}\right). \quad (27)$$

Hence, the imaginary part of the modified potential in the anisotropic medium is given as

$$\mathrm{Im}[V(r,\theta_r,T)] = \frac{\alpha s^2 T}{3}\left\{\frac{\xi}{60}(7-9\cos 2\theta_r)-1\right\}\log\left(\frac{1}{s}\right) + \frac{s^4\sigma T}{m_D^2}\left\{\frac{\xi}{35}\left(\frac{1}{9}-\frac{1}{4}\cos 2\theta_r\right)-\frac{1}{30}\right\} \times \log\left(\frac{1}{s}\right). \quad (28)$$

C. Binding energy (E_b) and thermal width (Γ)

While considering the small anisotropy, one can solve the Schrödinger equation and obtain the real part of the binding energy (BE or E_b) by just considering the isotropic part with the first order perturbation in anisotropy parameter ξ, as done in [80–82]. In this case, the real part of E_b is

$$\mathrm{Re}[E_b(T)] = \left(\frac{m_Q\sigma^2}{m_D^4 n^2}+\alpha m_D+\frac{\xi}{3}\left(\frac{m_Q\sigma^2}{m_D^4 n^2} + \alpha m_D+\frac{2m_Q\sigma^2}{m_D^4 n^2}\right)\right). \quad (29)$$

In the small-distance limit, the imaginary part of the potential can be considered as a perturbation to the vacuum potential [82], which provides an estimate for the thermal width for a particular resonance state, given as

$$\Gamma(T) = -\int d^3\mathbf{r}|\Psi(r)|^2\mathrm{Im}V(\mathbf{r}). \quad (30)$$

The medium potential, at high temperature, has a long-range Coulombic tail that dominates over all the other terms. Owing to this fact, one can choose the $\Psi(r)$ as the Coulombic wave function. The Coulombic wave function for the ground state [$1s$, corresponding to $n=1$ (J/ψ and Υ)] and the first excited state [$2s$, corresponding to $n=2$ (ψ' and Υ')], respectively, is given as

$$\Psi_{1s}(r) = \frac{1}{\sqrt{\pi a_0^3}}e^{\frac{-r}{a_0}}, \qquad \Psi_{2s}(r) = \frac{1}{4\sqrt{2\pi a_0^3}}\left(2-\frac{r}{a_0}\right)e^{\frac{-r}{2a_0}}, \quad (31)$$

where $a_0 = 2/(\alpha m_Q)$ is the Bohr radius of the quarkonia system. Now, using Eq. (30), we have

$$\Gamma_{1s/2s}(T) = m_D^2 T\int d^3\mathbf{r}|\Psi_{1s/2s}(r)|^2 \times\left[\frac{\alpha}{3}\left\{\frac{\xi}{60}(7-9\cos 2\theta_r)-1\right\} + \sigma r^2\left\{\frac{\xi}{35}\left(\frac{1}{9}-\frac{1}{4}\cos 2\theta_r\right)-\frac{1}{30}\right\}\right] \times r^2\log\left(\frac{1}{rm_D}\right). \quad (32)$$

We rewrite the above equation as

$$\Gamma_{1s}(T) = \left(\frac{\xi}{3}-2\right)m_D^2 T[\alpha I_1+\sigma I_2], \quad (33)$$

where

$$I_1 = \frac{12\log\left(\frac{\alpha m_Q}{m_D}\right)+12\gamma-25}{6\alpha^2 m_Q^2} \quad (34)$$

and

$$I_2 = \frac{3\left(20\log\left(\frac{\alpha m_Q}{m_D}\right)+20\gamma-49\right)}{10\alpha^4 m_Q^4}. \quad (35)$$

Ultimately, the thermal width for the $1s$-state appears as

$$\Gamma_{1s}(T) = \frac{m_D^2 T(\xi-6)}{90\alpha^4 m_Q^4}\left(60(\alpha^3 m_Q^2+3\sigma)\log\left(\frac{\alpha m_Q}{m_D}\right) + 5(12\gamma-25)\alpha^3 m_Q^2+9(20\gamma-49)\sigma\right). \quad (36)$$

It is important to note that in Ref. [82], while considering up to leading logarithmic order of the imaginary potential, the authors have taken the width up to leading logarithmic order as well. Thus, they consider the dissociation width of the following form for the $1s$-state,

$$\Gamma_{1s}(T) = T\left(\frac{4}{\alpha m_Q^2}+\frac{12\sigma}{\alpha^4 m_Q^4}\right)\left(1-\frac{\xi}{6}\right)m_D^2\log\left(\frac{m_D}{\alpha m_Q}\right). \quad (37)$$

In the present case, it has been observed that additional terms, other than the leading logarithmic term, also contribute significantly. Hence, we consider the full expression of the width given in Eq. (36). Note that the authors in Ref. [82] have taken the normalization constant C_ξ equal to unity, which is different in our case as it has a remarkable contribution. Hence, we have modified the expression, as one can see in Eq. (37) and other places as well.

For the $2s$-state, we have

$$\Gamma_{2s}(T) = \frac{T(\xi-6)}{45\alpha^2 m_Q^2}\left(35(12\gamma-31)\alpha+\frac{72(160\gamma-447)\sigma}{\alpha^2 m_Q^2} + 60\left(7\alpha+\frac{192\sigma}{\alpha^2 m_Q^2}\right)\log\left(\frac{\alpha m_Q}{2m_D}\right)\right)m_D^2, \quad (38)$$

and the leading logarithmic order for the $2s$-state is given as

$$\Gamma_{2s}(T) = \frac{8m_D^2 T}{\alpha^4 m_Q^4}\left(1-\frac{\xi}{6}\right)(7\alpha^3 m_Q^2+192\sigma)\log\left(\frac{2m_D}{\alpha m_Q}\right). \quad (39)$$

Again, in this case, we follow the solution given in Eq. (38) to calculate the binding energy.

Now, we have the real parts of the binding energies $E_b(T)$ (BE) as well as the thermal width $\Gamma(T)$ for both states. Exploiting the criteria discussed earlier, we can plot twice the binding energy along with the thermal width and obtain the dissociation temperature as the point of their intersection. In the next section, we discuss the important results in detail.

III. RESULTS AND DISCUSSION

In the present analysis, various quantities have been obtained, and the results are plotted while considering the weak anisotropy in the hot QCD plasma with the fixed critical temperature $T_c = 0.17$ GeV. We considered $\xi = -0.3$ for prolate and $\xi = 0.3$ for oblate, whereas for the isotropic case, we have $\xi = 0$. The EoSs that are employed here are symbolized as follows: The 3-loop HTL perturbative results are denoted with HTLpt, while the lattice results are shown as LB; LO refers to the leading order (ideal case or noninteracting case).

In Fig. 1, the real part of the medium modified potential has been plotted with respect to r, using Eq. (21), at temperature $T = 3T_c$ GeV. In the LO case, the potential is seen to be less negative, in contrast to nonideal cases, at both parallel, $\theta_r = 0$ (left panel), and perpendicular, $\theta_r = \pi/2$ (right panel), directions. For $\xi = 0.3$, the numbers are slightly larger as compared to $\xi = 0$. The numbers for the prolate case, $\xi = -0.3$, are found to be the smallest among them. For $\theta_r = \pi/2$, as compared to $\theta_r = 0$, the results are found to be similar but have slightly larger separation for different anisotropies. This shows that the real part of the potential is marginally affected by the presence of anisotropy, as one traverses from the longitudinal plane to the transverse plane. As mentioned earlier, we have obtained the Cornell form of the potential from the modified one in the limit $T \to 0$ and plotted it in the same figures [Figs. 1(a) and 1(b)] at $\alpha = 0.3$ and $\sigma = 0.184\,\mathrm{GeV}^2$.

In a similar way, the imaginary part of the medium modified potential, within the limit $rm_D \ll 1$ and considering the leading order in ξ, has been plotted in Fig. 2, with the same parameters as discussed in the case of the real part, using Eq. (28). For the smaller values of r, the imaginary part of the medium modified potential is found to be positive. As the effective radius increases, there is a crossover to the negative values. In both cases, $\theta_r = \pi/2$ and $\theta_r = 0$, the nonideal EoSs follow the same pattern as the ideal one. The effect of anisotropy is found to have less impact on the imaginary part of the potential as compared to the real one.

As discussed earlier, the dissociation temperature has been obtained by employing the following criterion: The temperature at which twice the binding energy (real part) equals the thermal width and causes dissociation of quarkonia is the dissociation temperature. In Figs. 3–5, respectively, the thermal width of J/ψ, Υ and Υ' have been plotted, along with twice the real part of their corresponding BE. In each case, LO is shown in the left panel, HTLpt in the middle panel, and LB in the right panel. To plot them, the masses for J/ψ, Υ and Υ' are taken as 3.096 GeV, 9.460 GeV and 10.023 GeV, respectively, as calculated in [97–99]. In all the plots, for the oblate case, $\xi = 0.3$, the intersection points are found to be larger as compared to the isotropic case, $\xi = 0$. The numbers for the prolate case, $\xi = -0.3$, are observed to be the least among them. The results for the various EoSs are shown separately in the tables. The LO results for different anisotropies are presented in Table I, 3-loop HTL perturbative calculation results are in Table II, and $(2+1)$-lattice results are shown in Table III. In the LO case, one can observe that the

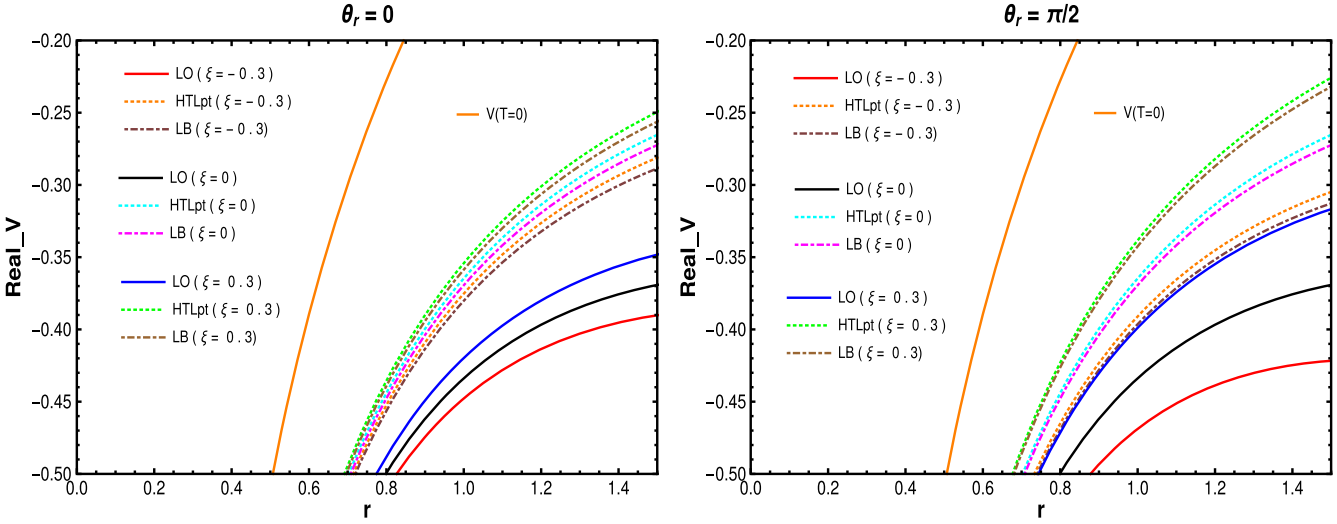

FIG. 1. Real part of the medium modified potential for $\theta_r = 0$ (left panel) and $\theta_r = \pi/2$ (right panel) with various EOSs and different ξ at fixed $T_c = 0.17$ GeV and $T = 3T_c$ GeV, along with the potential at $T = 0$.

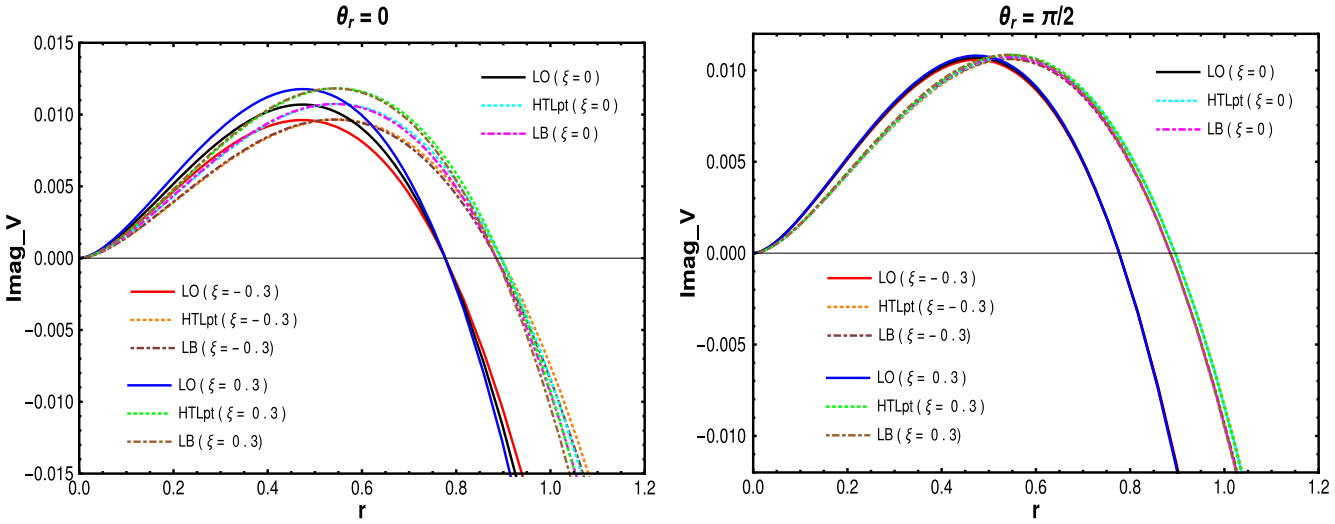

FIG. 2. Imaginary part of the medium modified potential for $\theta_r = 0$ (left panel) and $\theta_r = \pi/2$ (right panel) with various EOSs and different ξ at fixed $T_c = 0.17$ GeV and $T = 3T_c$ GeV.

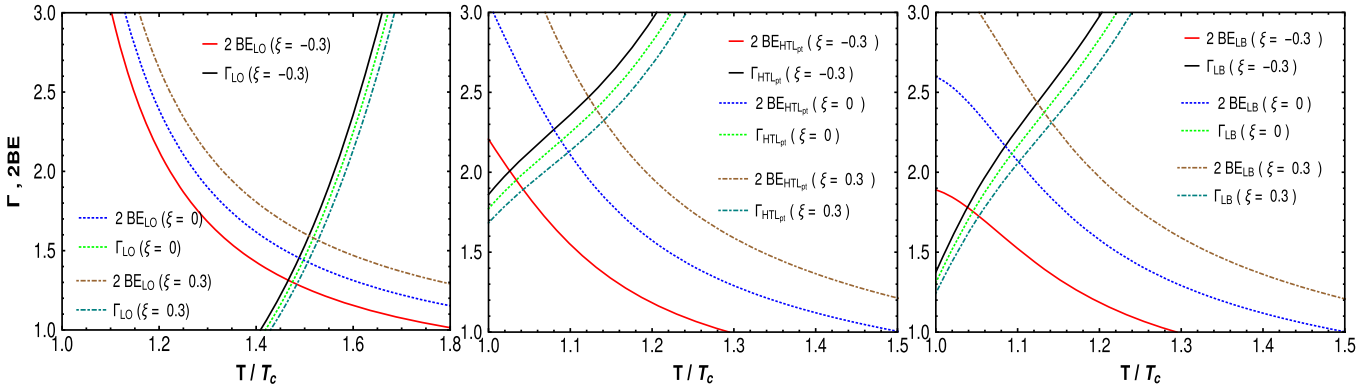

FIG. 3. Γ, 2BE (E_b) vs T/T_c for J/ψ at $T_c = 0.17$ GeV with different ξ. We have plotted the leading order (noninteracting) results (left panel) along with the 3-loop HTLpt (middle panel) and lattice (right panel).

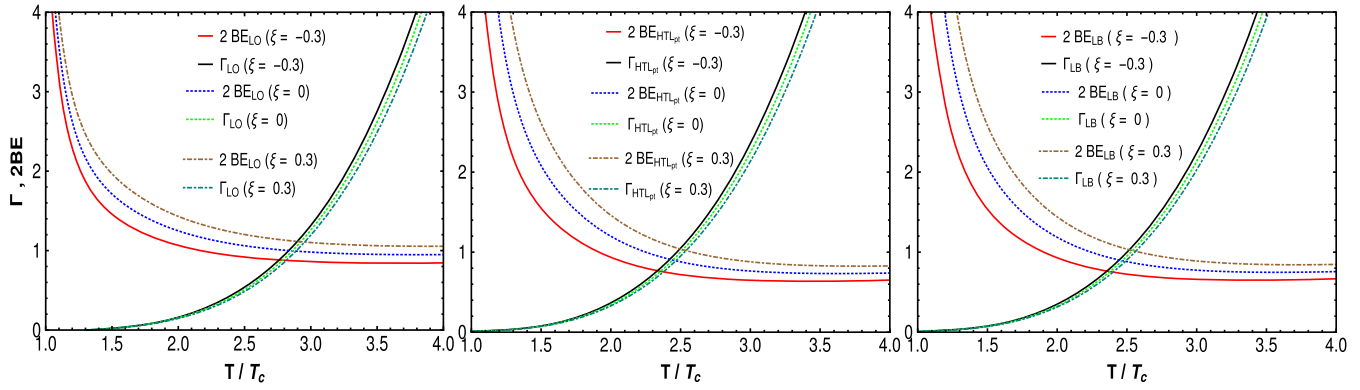

FIG. 4. Γ, 2BE (E_b) vs T/T_c for Υ at $T_c = 0.17$ GeV with different ξ. We have plotted the leading order (noninteracting) results (left panel) along with the 3-loop HTLpt (middle panel) and lattice (right panel).

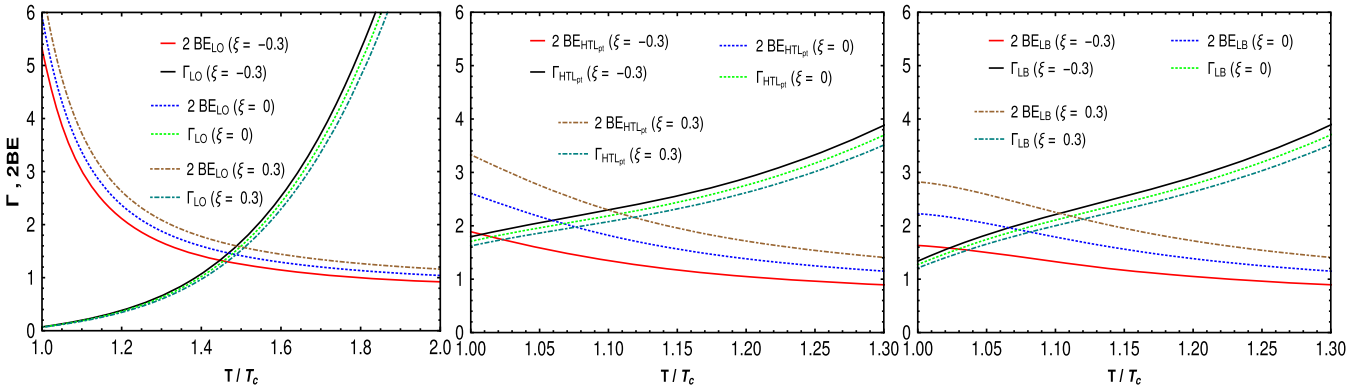

FIG. 5. Γ, 2BE (E_b) vs T/T_c for Υ' at $T_c = 0.17$ GeV with different ξ. We have plotted the leading order (noninteracting) results (left panel) along with the 3-loop HTLpt (middle panel) and lattice (right panel).

dissociation temperature is higher for Υ ($1s$-state) as compared to J/ψ ($1s$-state), while the excited state Υ' ($2s$-state) has the lowest dissociation temperature. This hierarchy has been observed in all three cases: oblate, prolate and isotropic.

A similar pattern is observed while taking the hot QCD medium effects into consideration, either through HTL perturbative results or lattice simulation results as shown in Tables II and III, respectively. But the essential point is that, as one gets closer to the realistic picture by including the hot QCD medium interaction effects, a decrease in dissociation temperature is observed. The nonideal EoSs have almost overlapping numbers, but to be more precise, the 3-loop HTLpt results are found to be the smallest among them.

TABLE I. Ideal (noninteracting EoS) results for the three cases: prolate, isotropic and oblate.

LO results			
	Temperature (in units of T_c)		
States ↓	$\xi = -0.3$	$\xi = 0.0$	$\xi = 0.3$
Υ	2.861	2.964	3.062
Υ'	1.447	1.478	1.508
J/ψ	1.487	1.520	1.551

TABLE II. HTL perturbative results for all three cases: prolate, isotropic and oblate.

3-loop HTLpt			
	Temperature (in units of T_c)		
States ↓	$\xi = -0.3$	$\xi = 0.0$	$\xi = 0.3$
Υ	2.427	2.540	2.639
Υ'	1.008	1.067	1.118
J/ψ	1.054	1.119	1.172

The numbers for dissociation temperatures are found to be consistent with those given in Refs. [82,84]. Specifically, while implementing the interacting EoSs, the numbers are observed to be closer. For each state, we displayed a contrast in Table IV by calculating the decrease [in percentage (%)] in the dissociation temperatures due to the presence of hot QCD medium effects. It is found that the dissociation temperatures, while incorporating hot QCD medium effects, have been lowered by around 13% to 31%. The excited state Υ' has been reduced twice as much as the ground state Υ.

TABLE III. Lattice simulation results for all three cases: prolate, isotropic and oblate.

Lattice, Bazabov (2014)			
	Temperature (in units of T_c)		
States ↓	$\xi = -0.3$	$\xi = 0.0$	$\xi = 0.3$
Υ	2.451	2.564	2.665
Υ'	1.023	1.074	1.120
J/ψ	1.063	1.121	1.172

TABLE IV. Drop in the dissociation temperature from LO results while applying HTLpt and lattice.

Change in percentage (%)			
Using HTLpt			
States ↓	$\xi = -0.3$	$\xi = 0.0$	$\xi = 0.3$
Υ	15.2	14.3	13.8
Υ'	30.3	27.8	25.9
J/ψ	29.1	26.7	24.4
Using lattice			
Υ	14.3	13.5	13.0
Υ'	29.3	27.3	25.7
J/ψ	28.5	26.6	24.4

Note that we also tried for ψ' ($2s$-state, whose mass is 3.686 GeV) but did not find any intersection point above the critical temperature (T_c). Based on the earlier discussion, this behavior is expected because the excited states decay at lower temperatures than their corresponding ground state (J/ψ, which is found to decay at very close to T_c). A similar suppression pattern has already been seen in the case of Υ' and Υ.

IV. SUMMARY AND CONCLUSION

The dissociation temperatures for the bottonium and the charmonium [ground ($1s$) as well as first excited ($2s$)] states have been obtained using the medium modified interquark potential in the anisotropic hot QCD medium. The real or imaginary part of the heavy-quark potential is obtained in terms of the real or imaginary part of the complex permittivity. The real part of the medium modified potential causes a dynamical screening of color charge that leads to the temperature-dependent binding energy, whereas the imaginary part of the same potential leads to the temperature-dependent thermal dissociation width. It has been observed that with the increase in temperature, the binding energy of the heavy quarkonia decreases, while the thermal dissociation width increases. Exploiting the criteria employed here, the dissociation temperature for each state has been calculated, where twice the binding energy equals the thermal dissociation width.

The hot QCD medium interaction effects have been incorporated through the Debye mass by employing the EQPM. Considering the above fact, the Debye mass has been normalized in both mediums to make it immune from the effects of the anisotropy so that the impact of various EoSs can be seen clearly. After incorporating the medium interaction effects, the results are found to be smaller in magnitude as compared to the noninteracting or weakly interacting, ideal one. We further note that the finite momentum-space anisotropy in the prolate $\xi < 0$ case decreases, while in the oblate $\xi > 0$ case, the dissociation temperature increases as compared to the isotropic one, $\xi = 0$, for all states taken into account. It has also been observed that in both the charmonium and bottonium cases, the excited states dissociate earlier (at low temperature) than their corresponding ground state. Furthermore, we have not found an intersection point above T_c for the ψ'-state. Finally, we observed that both the anisotropy and the hot QCD medium effects present in EoS play a significant role in deciding the fate of heavy-quarkonia states in the hot QCD/QGP medium.

To extend the present work, we aim to incorporate the viscous effects and study the dissociation of heavy quarkonia in hydrodynamically expanding viscous QGP. In addition, the collisional effects on the quarkonia suppression will be carried out in the near future.

ACKNOWLEDGMENTS

We would like to acknowledge the people of India for their generous support for the research in fundamental sciences in the country. I. N. acknowledges IIT Gandhinagar for the academic visit and hospitality during the course of this work. V. C. would like to acknowledge SERB, Govt. of India for the Early Career Research Award (ECRA/2016).

[1] J. Adams *et al.* (STAR Collaboration), Nucl. Phys. **A757**, 102 (2005); K. Adcox *et al.* (PHENIX Collaboration), Nucl. Phys. **A757**, 184 (2005); B. B. Back *et al.* (PHOBOS Collaboration), Nucl. Phys. **A757**, 28 (2005); I. Arsene *et al.* (BRAHMS Collaboration), Nucl. Phys. **A757**, 1 (2005).
[2] K. Aamodt *et al.* (Alice Collaboration), Phys. Rev. Lett. **105**, 252302 (2010); **105**, 252301 (2010); **106**, 032301 (2011).
[3] U. W. Heinz, arXiv:hep-ph/0407360.
[4] L. McLerran, Rev. Mod. Phys. **58**, 1021 (1986).
[5] L. D. Landau and E. M. Lifshitz, *Electrodynamics of Continuous Media* (Butterworth-Heinemann, Oxford, UK, 1984).
[6] M. C. Chu and T. Matsui, Phys. Rev. D **39**, 1892 (1989).
[7] Y. Koike, AIP Conf. Proc. **243**, 916 (1992).
[8] J. J. Aubert *et al.* (E598 Collaboration), Phys. Rev. Lett. **33**, 1404 (1974).
[9] J. E. Augustin *et al.* (SLAC-SP-017 Collaboration), Phys. Rev. Lett. **33**, 1406 (1974).
[10] T. Matsui and H. Satz, Phys. Lett. B **178**, 416 (1986).
[11] A. Mocsy and P. Petreczky, Euro. Phys. J. C **43**, 77 (2005); Phys. Rev. D **73**, 074007 (2006).
[12] V. Agotiya, V. Chandra, and B. K. Patra, Phys. Rev. C **80**, 025210 (2009).
[13] B. K. Patra, V. Agotiya, and V. Chandra, Eur. Phys. J. C **67**, 465 (2010).
[14] S. Datta, F. Karsch, P. Petreczky, and I. Wetzorke, Phys. Rev. D **69**, 094507 (2004).
[15] N. Brambilla, J. Ghiglieri, P. Petreczky, and A. Vairo, Phys. Rev. D **78**, 014017 (2008).
[16] Y. Burnier, M. Laine, and M. Vepsáláinen, Phys. Lett. B **678**, 86 (2009).
[17] A. Dumitru, Y. Guo, and M. Strickland, Phys. Rev. D **79**, 114003 (2009).
[18] M. Laine, O. Philipsen, P. Romatschke, and M. Tassler, J. High Energy Phys. 03 (**2007**) 054.
[19] E. Eichten, S. Godfrey, H. Mahlke, and J. L. Rosner, Rev. Mod. Phys. **80**, 1161 (2008).

[20] M. B. Voloshin, Prog. Part. Nucl. Phys. **61**, 455 (2008).
[21] C. Patrignani, T. K. Pedlar, and J. L. Rosner, Annu. Rev. Nucl. Part. Sci. **63**, 21 (2013);
[22] N. Brambilla *et al.*, Eur. Phys. J. C **71**, 1534 (2011).
[23] A. D. Frawley, T. Ullrich, and R. Vogt, Phys. Rep. **462**, 125 (2008).
[24] E. L. Berger, J. w. Qiu, and Y. l. Wang, Phys. Rev. D **71**, 034007 (2005).
[25] J. F. Amundson, O. J. P. Eboli, E. M. Gregores, and F. Halzen, Phys. Lett. B **390**, 323 (1997).
[26] L. Adamczyk *et al.* (STAR Collaboration), Phys. Lett. B **722**, 55 (2013).
[27] E. L. Berger and D. L. Jones, Phys. Rev. D **23**, 1521 (1981).
[28] R. Rapp, D. Blaschke, and P. Crochet, Prog. Part. Nucl. Phys. **65**, 209 (2010).
[29] C. Silvestre (PHENIX Collaboration), J. Phys. G **35**, 104136 (2008).
[30] F. Scardina, M. Colonna, S. Plumari, and V. Greco, Phys. Lett. B **724**, 296 (2013).
[31] G. T. Bodwin, E. Braaten, and G. P. Lepage, Phys. Rev. D **51**, 1125 (1995); **55**, 5853 (1997).
[32] W. E. Caswell and G. P. Lepage, Phys. Lett. **167B**, 437 (1986).
[33] A. Pineda, Prog. Part. Nucl. Phys. **67**, 735 (2012).
[34] H. S. Shao, H. Han, Y. Q. Ma, C. Meng, Y. J. Zhang, and K. T. Chao, J. High Energy Phys. 05 (2015) 103.
[35] E. Eichten, K. Gottfried, T. Kinoshita, K. D. Lane, and T. M. Yan, Phys. Rev. D **17**, 3090 (1978).
[36] E. Eichten, K. Gottfried, T. Kinoshita, K. D. Lane, and T. M. Yan, Phys. Rev. D **21**, 203 (1980).
[37] H. S. Chung, J. Lee, and D. Kang, J. Korean Phys. Soc. **52**, 1151 (2008).
[38] A. V. Luchinsky, arXiv:1709.02444; Mod. Phys. Lett. A **33**, 1850001 (2018).
[39] B. Fulsom, arXiv:1710.00120.
[40] J. Soto, arXiv:1709.08038.
[41] P. Faccioli, C. Loureno, M. Arajo, V. Knnz, I. Krtschmer, and J. Seixas, Phys. Lett. B **773**, 476 (2017).
[42] T. Song, J. Aichelin, and E. Bratkovskaya, Phys. Rev. C **96**, 014907 (2017).
[43] S. T. Araya (ATLAS Collaboration), Nucl. Part. Phys. Proc. **289–290**, 393 (2017).
[44] A. Adare *et al.* (PHENIX Collaboration), Phys. Rev. C **84**, 054912 (2011).
[45] C. Gale, S. Jeon, and J. I. Kapusta, Nucl. Phys. **A661**, 558 (1999).
[46] C. Gale, S. Jeon, and J. I. Kapusta, Phys. Lett. B **459**, 455 (1999).
[47] P. Rosnet (ALICE Collaboration), Proc. Sci. **DIS2017**, 128 (2018).
[48] A. Szczurek, A. Cisek, and W. Schafer, arXiv:1710.11450.
[49] J. A. López López (ATLAS Collaboration), Nucl. Phys. **A967**, 584 (2017).
[50] Q. Hu (ATLAS Collaboration), Nucl. Phys. **A956**, 685 (2016).
[51] J. Nachtman, *Proc. Sci.*, ICHEP2016 (2017) 608.
[52] A. Szczurek, A. Cisek, and W. Schafer, Acta Phys. Pol. B **48**, 1207 (2017).
[53] K. Müller (LHCb Collaboration), J. Phys. Conf. Ser. **878**, 012011 (2017).
[54] A. K. Likhoded, A. V. Luchinsky, and S. V. Poslavsky, JETP Lett. **105**, 739 (2017).
[55] S. Aronson, E. Borras, B. Odegard, R. Sharma, and I. Vitev, Phys. Lett. B **778**, 384 (2018).
[56] A. Cisek and A. Szczurek, arXiv:1711.00377.
[57] D. Thakur, S. De, R. Sahoo, and S. Dansana, Phys. Rev. D **97**, 094002 (2018).
[58] S. Chen and M. He, Phys. Rev. C **96**, 034901 (2017).
[59] M. Abu-Shady, T. A. Abdel-Karim, and E. M. Khokha, Adv. High Energy Phys. 7356843 (2018).
[60] H. Negash and S. Bhatnagar, Adv. High Energy Phys. **2017**, 1 (2017).
[61] N. R. F. Braga and L. F. Ferreira, Phys. Rev. D **94**, 094019 (2016).
[62] B. Duclou, T. Lappi, and H. Mntysaari, Nucl. Part. Phys. Proc. **289–290**, 309 (2017).
[63] N. Brambilla, A. Pineda, J. Soto, and A. Vairo, Rev. Mod. Phys. **77**, 1423 (2005); N. Brambilla, M. A. Escobedo, J. Ghiglieri, and A. Vairo, J. High Energy Phys. 05 (2013) 130.
[64] J. Geiss, C. Greiner, E. L. Bratkovskaya, W. Cassing, and U. Mosel, Phys. Lett. B **447**, 31 (1999).
[65] V. K. Agotiya, V. Chandra, M. Y. Jamal, and I. Nilima, Phys. Rev. D **94**, 094006 (2016).
[66] P. Romatschke, Phys. Rev. C **75**, 014901 (2007); P. Romatschke and M. Strickland, Phys. Rev. D **71**, 125008 (2005).
[67] B. Schenke and M. Strickland, Phys. Rev. D **76**, 025023 (2007).
[68] M. Martinez and M. Strickland, Phys. Rev. Lett. **100**, 102301 (2008); Phys. Rev. C **78**, 034917 (2008).
[69] A. Dumitru, Y. Nara, B. Schenke, and M. Strickland, Phys. Rev. C **78**, 024909 (2008).
[70] R. Baier and Y. Mehtar-Tani, Phys. Rev. C **78**, 064906 (2008).
[71] A. Dumitru, Y. Guo, and M. Strickland, Phys. Lett. B **662**, 37 (2008).
[72] M. E. Carrington and A. Rebhan, Phys. Rev. D **79**, 025018 (2009).
[73] V. Chandra, R. Kumar, and V. Ravishankar, Phys. Rev. C **76**, 054909 (2007); **76**, 069904(E) (2007); V. Chandra, A. Ranjan, and V. Ravishankar, Eur. Phys. J. A **40**, 109 (2009).
[74] V. Chandra and V. Ravishankar, Phys. Rev. D **84**, 074013 (2011).
[75] P. Romatschke and M. Strickland, Phys. Rev. D **68**, 036004 (2003).
[76] M. E. Carrington, K. Deja, and S. Mrowczynski, Phys. Rev. C **90**, 034913 (2014).
[77] M. Yousuf, S. Mitra, and V. Chandra, Phys. Rev. D **95**, 094022 (2017).
[78] A. Beraudo, J. P. Blaizot, and C. Ratti, Nucl. Phys. **A806**, 312 (2008).
[79] M. Laine, O. Philipsen, and M. Tassler, J. High Energy Phys. 09 (2007) 066; T. Hatsuda, Nucl. Phys. **A904**, 210c (2013).
[80] M. Margotta, K. McCarty, C. McGahan, M. Strickland, and D. Yager-Elorriaga, Phys. Rev. D **83**, 105019 (2011).
[81] M. Strickland and D. Bazow, Nucl. Phys. **A879**, 25 (2012).
[82] L. Thakur, U. Kakade, and B. K. Patra, Phys. Rev. D **89**, 094020 (2014).

[83] Y. Burnier, M. Laine, and M. Vepsalainen, J. High Energy Phys. 01 (2008) 043.
[84] A. Mocsy and P. Petreczky, Phys. Rev. Lett. **99**, 211602 (2007).
[85] M. A. Escobedo and J. Soto, Phys. Rev. A **78**, 032520 (2008).
[86] M. Laine, Nucl. Phys. **A820**, 25C (2009).
[87] A. Bazabov *et al.*, Phys. Rev. D **90**, 094503 (2014).
[88] S. Borsanyi, Z. Fodor, C. Hoelbling, S. D. Katz, S. Krieg, and K. K. Szabó, Phys. Lett. B **730**, 99 (2014).
[89] N. Haque, A. Bandyopadhyay, J. O. Andersen, M. G. Mustafa, M. Strickland, and N. Su, J. High Energy Phys. 05 (2014) 027.
[90] J. O. Andersen, N. Haque, M. G. Mustafa, and M. Strickland, Phys. Rev. D **93**, 054045 (2016).
[91] A. Rothkopf, T. Hatsuda, and S. Sasaki, Phys. Rev. Lett. **108**, 162001 (2012).
[92] M. Laine and Y. Schroder, J. High Energy Phys. 03 (2005) 067.
[93] M. H. Thoma, arXiv:hep-ph/0010164.
[94] E. Braaten and R. D. Pisarski, Nucl. Phys. **B337**, 569 (1990).
[95] J. P. Blaizot and E. Iancu, Nucl. Phys. **B417**, 608 (1994).
[96] P. F. Kelly, Q. Liu, C. Lucchesi, and C. Manuel, Phys. Rev. D **50**, 4209 (1994).
[97] V. M. Aulchenko *et al.* (KEDR Collaboration), Phys. Lett. B **573**, 63 (2003).
[98] A. S. Artamonov *et al.*, Phys. Lett. **137B**, 272 (1984).
[99] D. P. Barber *et al.*, Phys. Lett. **135B**, 498 (1984).